

Preparation, electronic structure and optical properties of Na₂GeSe₃ crystals

D.I. Bletskan, V.V. Vakulchak*, I.L. Mykaylo, O.A. Mykaylo

Uzhhorod National University, 54, Voloshin str., 88000 Uzhhorod, Ukraine

*Corresponding author e-mail: vasyi.vakulchak@uzhnu.edu.ua

Abstract. From the first principles, in the framework of the density functional theory in LDA and LDA+*U* approximations, the band structure, total and partial densities of electronic states, spatial distribution of the electron charge density, also the optical functions: dielectric constant, refractive and absorption indices, reflection and absorption coefficients of Na₂GeSe₃ crystal have been calculated. According to the calculation results, Na₂GeSe₃ is a direct-gap crystal with the top of valence band and the bottom of conduction band at the point Γ of Brillouin zone. The calculated band gap is $E_{gd} = 1.7$ eV LDA and $E_{gd} = 2.6$ eV in the LDA+*U* approximations. Based on the data of total and partial densities of electronic states, contributions of atomic orbitals to the crystalline ones have been determined. Also, the data of chemical bond formation in the crystals under discussion have been obtained.

Keywords: crystal structure, crystal growth, computer simulation, electronic structure, absorption edge, optical functions.

<https://doi.org/10.15407/spqeo25.01.019>

PACS 31.15.E-, 71.15.Mb, 71.20.-b, 78.20.Ci, 81.10.-h

Manuscript received 05.11.21; revised version received 10.01.22; accepted for publication 22.03.22; published online 24.03.22.

1. Introduction

Currently, intensive work on finding electrode materials for sodium-ion batteries, which could potentially replace lithium-ion batteries has been underway [1]. A significant advantage of sodium-ion batteries compared to lithium ones is that there is much more sodium on Earth than lithium, therefore, sodium batteries could be cheaper than the lithium ones. Solid electrolytes are also needed to create sodium batteries [2]. Promising materials with high ionic conductivity based on sodium cations at room temperature are ternary glasses known in the systems Na–Ge–S(Se) [3, 4]. For the presence of ionic conductivity, it is necessary to have “tunnels” in the crystal lattice of the matrix, along which alkali metal ions move. Among these materials is sodium selenogermanate (Na₂GeSe₃).

For a long time, information on phase equilibria and the formation of compounds in the Na₂Se–GeSe₂ system was absent in literature. The author of [5] succeeded to synthesize only four alloys in the Na₂Se–GeSe₂ system containing 10, 20, 30, and 40 wt.% Na₂Se. Alloys containing 10 and 20 wt.% of Na₂Se were obtained in a crystalline state, and those containing 30 and 40 wt.% Na₂Se – in a glassy state. The author [5] carried out the

synthesis of alloys by fusion of sodium selenide and germanium diselenide. Later, Na₂GeSe₃ [6] and Na₂Ge₂Se₅ [7] crystals were synthesized and their crystal structure was studied.

Prospects for practical application of materials based on solid electrolytes are defined by the degree of understanding the nature of physicochemical properties formation and finding interactions of their purposeful modification. The solution to such problems requires a detailed study of the electronic structure and chemical bonds of ternary compounds known in the Na₂Se–GeSe₂ system. Up to date, the electronic structure and optical properties have been studied only for Na₂Ge₂Se₅ [7, 8]. It should be noted that Na₂Ge₂Se₅ crystals exhibit strong nonlinear optical (NLO) second harmonic generation responses in the visible and infrared regions.

In this paper, an original method of synthesizing and growing the ternary compound Na₂GeSe₃ is described, as well as the results of studying the edge absorption spectrum. Using the density functional method in LDA and LDA+*U* approximations, we calculated the energy band structure, total and local partial densities of states, spatial distribution of the electron density and the optical functions of Na₂GeSe₃ crystal.

2. Synthesis of compound and crystal growth

2.1. The synthesis of the compound

The direct synthesis of Na_2GeSe_3 compound by fusion of elementary components is difficult because of high reactivity inherent to the alkali metal and the explosive nature of sodium-selenium interaction. A more acceptable preparation method of sodium seleno-germanate is fusing stoichiometric amounts of Na_2Se and GeSe_2 in evacuated silica ampoules. However, during the reaction, sodium selenide partially interacts with the walls of silica ampoule, thereby leading to a violation of stoichiometry and contamination of the ternary compound.

To obtain a single-phase and a high degree of purity for the ternary compound Na_2GeSe_3 suitable for growing high-quality single crystals, and to avoid the explosion hazard of the synthesis process, two new synthesis methods have been proposed (Fig. 1). According to the first method, the Na_2GeSe_3 compound was obtained by fusion of a stoichiometric amount of the alkali metal (Na), mono- or diselenide of germanium and selenium, loaded in layers into an alundum crucible (2). The alundum crucible with starting materials was placed inside the silica ampoule (1), after which it was pumped out to the pressure of 0.1 Pa and sealed (Fig. 1a). The necessity of layered loading of starting materials in the crucible is caused by the high reactivity of the alkali metal and the explosive nature of its interaction with selenium. Considering that germanium mono- and diselenide reacts actively with sodium, this leads to the strong local heating, accompanied by the destruction of the alundum crucible at the alkali metal – germanium mono- or diselenide boundary. For this reason, it is necessary to isolate the alkali metal during the synthesis both from selenium and the alundum crucible walls. This problem was solved using the second synthesis method of the ternary compound Na_2GeSe_3 . To protect the alkali metal from direct contact with selenium, interaction between which leads to the destruction of the alundum crucible and the explosion of the ampoule, special crucibles were made from germanium diselenide (Fig. 2), inside of which the alkali metal was placed (Fig. 1b).

According to the second method, initially, selenium (3) was loaded into the alundum crucible (2), then germanium diselenide crucible (4) with sodium (5) in it. Then, the silica ampoule (1) was evacuated down to 0.1 Pa and sealed (Fig. 1b). All preparatory operations, weighing of the starting materials, loading them into ampoules were carried out in a chamber of a purified argon atmosphere, to prevent the interaction of the alkali metal with air and moisture.

It should be noted that specially made crucibles from germanium monoselenide were also successfully used for the synthesis since the interaction of GeSe with sodium was less aggressive than in the case of germanium diselenide.

The synthesis of compounds was carried out in a vertical dual-zone resistance tube furnace, providing a temperature gradient along the ampoule, with the aim of

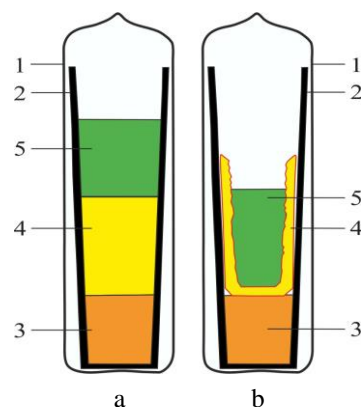


Fig. 1. The location of starting components for synthesizing the Na_2GeSe_3 crystals in accord with the first method (a) and the second one (b). 1 – silica tube, 2 – alundum crucible, 3 – selenium, 4 – germanium diselenide crucible, 5 – sodium.

heating the upper part of the ampoule (the alkali metal location zone) higher than the lower ampoule part (selenium location zone).

The synthesis was carried out in three stages. At the first stage, the initial substances were heated to the temperature 10...25 K higher than the sodium melting temperature at the rate of 10...15 K/h, then keeping it in the furnace for 15...20 hours. The temperature gradient was 8...10 K/cm. Such heating rates and exposure ensured the slow reaction rate and complete sodium interaction. It interacted mainly with germanium mono- or diselenide, but not directly with selenium, which avoided a violent exothermic reaction and excluded the ampoule explosion. The presence of the temperature gradient slowed down the diffusion of selenium to sodium through the bottom of crucibles from germanium mono- or diselenide.

At the second stage, the temperature was increased to 910...920 K at the rate of 50...60 K/h and kept for 3...4 hours, which was sufficient for the complete interaction of selenium. After that, at the third stage, the temperature gradient in the furnace was reduced to 3...5 K/cm for 1...2 hours, and the temperature was increased up to 110 K with the rate of 90...100 K/h and

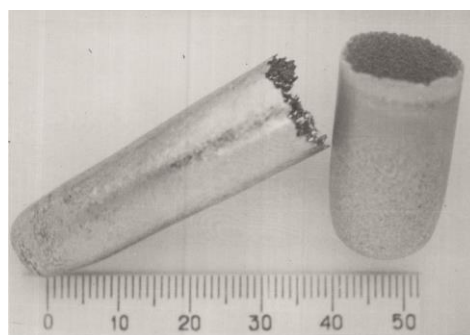


Fig. 2. Forms of germanium selenide crucibles (GeSe and GeSe_2).

kept for 1.5...2 hours. This gradient was sufficient for steady heating the batch and at the same time prevented sublimation of the substance from the alundum crucible into the upper part of the silica ampoule, and the temperature regime ensured the complete reaction. Cooling the substance was carried out at the rate of 100...120 K/h down to 750...770 K, then kept at this temperature for 160 hours, and cooled to the room temperature in an off mode furnace.

The described method of synthesis Na_2GeSe_3 compound allows us to avoid the disadvantages of previously known methods, and to obtain a high-purity stoichiometric compound, also to eliminate the explosion hazard of the synthesis.

2.2. Preparation of crucibles from germanium chalcogenides

Preparation of crucibles from germanium mono- or diselenide is based on vacuum sublimation of these compounds in evacuated silica ampoules of appropriate dimensions. The required amount of germanium mono- or diselenide (4...7 g) was loaded into the silica ampoule, the inner diameter of which corresponded to the inner diameter of the alundum crucible in which Na_2GeSe_3 compound was synthesized. The silica ampoule with the starting material was evacuated down to 0.1 Pa and sealed, then it was placed in the horizontal dual-zone resistance furnace. Polycrystalline germanium mono- or diselenide (1) was located in the hot zone (2), where it sublimated, and at the bottom and walls of the ampoule (4) in the cold zone (3) it condensed with the crucible formation (5) (Fig. 3). The temperature of the hot zone was 880...900 K and in the cold zone – 800...820 K. During the sublimation process, the ampoules were simultaneously rotated and moved in the furnace. Visualization of the crucible formation process, rotation, and movement of the ampoule in the furnace enabled to vary the wall and bottom thicknesses, and crucible dimensions ($0 = 10...15$ mm, $1 = 20...50$ mm, wall and bottom thicknesses 1...2 mm).

After crucible formation, the ampoule was cooled in air, and then in the flame of gas burner (carefully, not leading to melting). The formed crucibles from GeSe or GeSe₂ were heated, which facilitated its separation from the walls of ampoule. The ampoule was broken and the crucible of germanium mono- or diselenide extracted (Fig. 2).

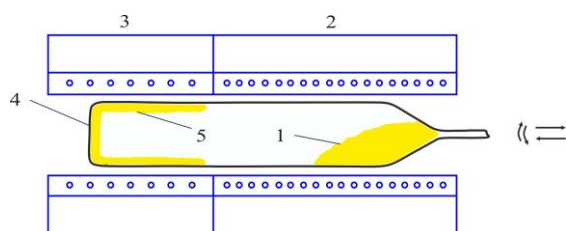


Fig. 3. Preparation scheme for germanium chalcogenide crucibles.

2.3. Crystal growth

Single crystals were grown using directional crystallization of the melt by the Bridgman–Stockbarger method in a vertical dual-zone resistance furnace.

At the first stage, the formation process providing the growth of crystallization center was carried out. With this aim, the ampoule with the charge was evacuated down to 0.1 Pa, then placed in the hot zone ($T = 856$ K) of a growth furnace and completely melted. Further, the ampoule with the melt was moved down (to the cold zone), where the cooling of the melt lower part occurred and crystallization of the substance began. Since Na_2GeSe_3 compound is characterized by significant undercooling, formation of the single-crystal seed was provided in the following way. By moving the ampoule with the melt down (from the hot zone to the cold one), spontaneous crystallization of the melt part was achieved. Then, the ampoule was moved back to the hot zone with a temperature exceeding the melting point of the compound and the spontaneously crystallized region was etched, until its length was 3...5 mm. Recrystallization annealing was carried out for 24...48 hours, at the end of which a stepwise growth of the substance was carried out on the resulting seed at the rate close to 0.1...0.15 mm/h. The growth was stopped, when the crystallization front reached the capillary part of the growth ampoule.

At the second stage, the single crystal was grown by moving the furnace at the rate of 0.25...0.6 mm/h, with the temperature gradient reaching 4...5 K/mm. Upon completion of the full crystallization process, in order to avoid cracks and possible internal stresses of the single crystal, the annealing process was carried out in the crystallization zone for 80...100 h. Cooling to room temperature was performed at a rate not higher than 10 K/h.

Using the method of differential thermal analysis (DTA), the melting temperature ($T_m = 850$ K) and crystallization one ($T_{cr} = 795$ K) of obtained Na_2GeSe_3 single crystals were determined. The method of differential scanning calorimetry (DSC) is used to determine the melting enthalpy ($\Delta H = 30.3$ kJ/mol), and then the melting entropy ($\Delta S = 35.6$ J/K·mol) was calculated.

2.4. Crystal structure

X-ray diffraction studies of Na_2GeSe_3 crystals that we have grown confirmed that this compound crystallized in a monoclinic structure, the symmetry of which is described by $P2_1/c$ space group, which was previously reported in [6]. The unit cell contained four formula units ($Z = 4$) with lattice parameters $a = 7.097$, $b = 16.068$, $c = 6.073$ Å [6]. The experimentally measured density was $\rho_{exp} = 3.76$ g/cm³, the calculated one – $\rho_{cal} = 3.72$ g/cm³. In the unit cell, NaI, NaII, Ge, Se1, Se2, Se3 atoms occupy 4e positions with the coordinates: (0.78060; 0.47380; 0.16640), (0.56890; 0.83460; 0.02820), (0.02680; 0.17030; 0.34020), (0.19590; 0.56150; 0.33720), (0.94070; 0.30630; 0.17790), (0.62690; 0.64720; 0.05640). Ge atoms are in tetrahedral environment with selenium atoms. The framework of the crystalline structure is formed by endless chains

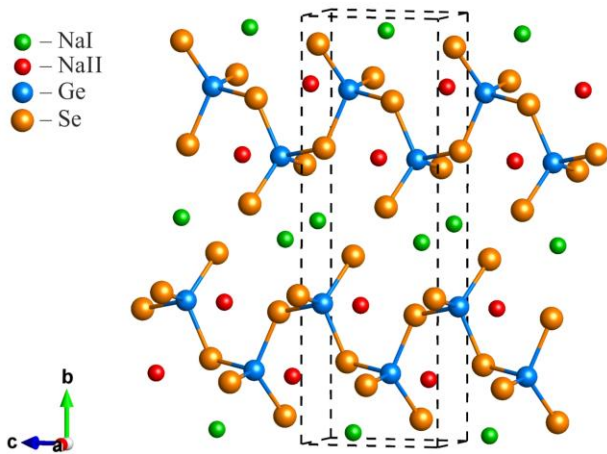


Fig. 4. The crystal structure of Na_2GeSe_3 .

$\langle \text{GeSe}_3 \rangle_n^{2n-}$ elongated along c axis, between which there are channel voids. The motif from which the chains are built is formed by two tetrahedra $[\text{GeSe}_4]$, interconnected by common vertices, having α -cis mutual orientation (Fig. 4), which determines the zigzag nature of chains. The unit cell contains two types of non-equivalent chains that differ in the opposite direction of twisting. The interatomic distances in Ge–Se chains (bridging) are 2.37...2.39 Å, Ge–Se (non-bridging) 2.30...2.31, Ge–Ge 3.97 Å, and the Se–Ge–Se bond angle is 95.71...117.31°. Thus, at the fusion of GeSe_2 and Na_2Se binary compounds in the 1:1 ratio there is the destruction of double tetrahedra $[\text{Ge}_2\text{Se}_6]$ characteristic of germanium diselenide [9], which linking endless tetrahedral chains into three-layer packets. That finally leads to formation only of Na_2GeSe_3 chain structure. In the voids between the chains, there are Na atoms in two nonequivalent positions: octahedral (NaI) and pentagramal (NaII). The latter (this polyhedron) can be described as a distorted trigonal bipyramid. The average NaI–Se distances are 2.91 Å, and NaII–Se 3.19 Å, respectively.

3. Method for calculation

The electronic structure and optical functions of Na_2GeSe_3 were calculated in the framework of the electron density functional theory [10] in the LDA and LDA+ U approximations [11] by using the SIESTA software package [12]. As a fundamental calculation basis, linear combinations of atomic orbitals were used. The periodic structure of the crystal was taken into account through the boundary conditions of the unit cell. The first-principle atomic norm-conserving pseudopotentials were used [13] in the calculation for electronic configurations: for Ge atoms – $[\text{Ar}] 4s^2 4p^2$, Se – $[\text{Ar}] 4s^2 4p^4$ and Na – $[\text{Ne}] 3s^1$ atoms. The indicated states relate to valence shells and $[\text{Ar}]$, $[\text{Ne}]$ relates to the core. The $4s$ -, $4p$ - and $4d$ -orbitals of germanium and selenium atoms and the $3s$ -, $3p$ - and $3d$ -orbitals of sodium atoms were included in the basic set of atomic orbitals of this compound.

The cut-off energy of atomic orbitals for a self-consistent calculation (SCF) was chosen so that to obtain convergence in the total energy of the cell no worse than 0.001 Ry/atom and was equal to $E_{cut} = 200$ Ry. The basis counted about 22320 atomic orbitals. The grid density of k -points in reciprocal space for the self-consistent calculation was chosen for the same reasons. The electron density was calculated by interpolation between $5 \times 3 \times 6$ grid nodes in reciprocal space. The total and partial densities of electronic states were determined using the modified tetrahedron method, for which the energy spectrum and wave functions were calculated on the k -grid containing 90 points. Integration over the irreducible part of the Brillouin zone was carried out using the special k -point method [14].

4. Results and discussion

4.1. Electronic structure and nature of the corresponding electronic states

The band structure of Na_2GeSe_3 crystal was calculated at the points of high symmetry Γ , B, D, Z, C, Y, A, E and along the lines between them in the Brillouin zone (BZ). It is shown in Fig. 5. The band structure of Na_2GeSe_3 calculated in LDA+ U approximation is shown in Fig. 6. The position of the top of the valence band located in the center of BZ at the point Γ was selected as the starting point in the energy scale. The bottom of conduction band also lies in the center of BZ, therefore sodium selenogermanate is a direct-gap crystal with the calculated band gap $E_{gd} = 1.7$ eV in LDA and $E_{gd} = 2.61$ eV in the LDA+ U approximations.

The correct choice of parameters corresponding to the one-center exchange-correlation of LDA+ U calculations for the electron band structure leads to results close to the experimental estimation of the band gap in comparison with calculations using LDA approximation.

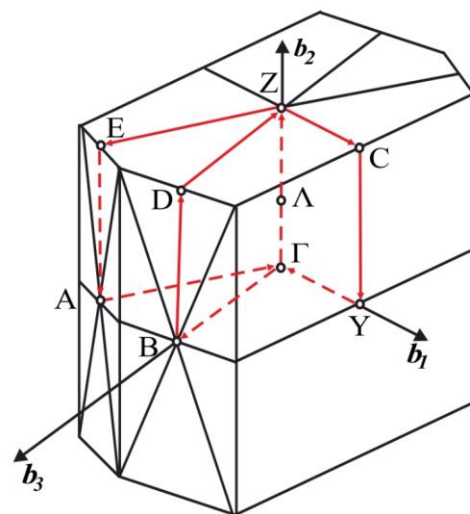


Fig. 5. The first Brillouin zone for the monoclinic lattice with distinguished points of symmetry and the way along which the band structure was calculated.

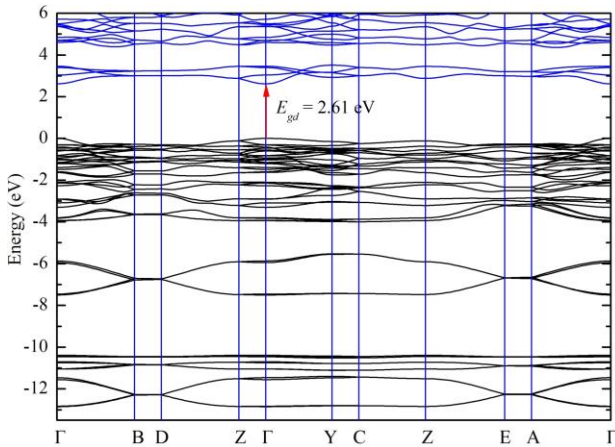


Fig. 6. The electron structure of monoclinic Na_2GeSe_3 (LDA+U).

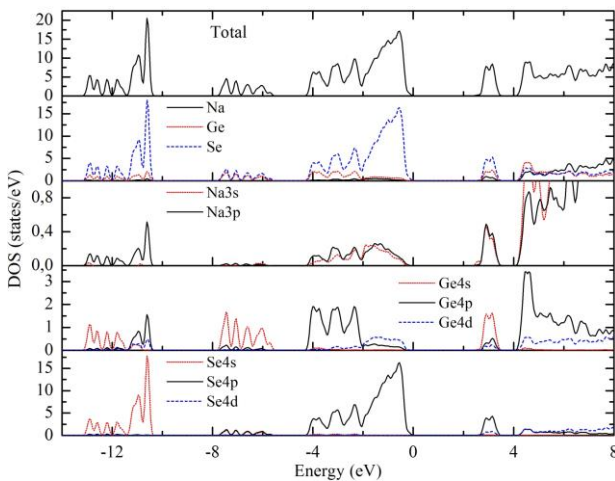


Fig. 7. The total and local partial densities of electron states in the Na_2GeSe_3 (LDA+U) crystal.

The band gap value found from the LDA+U calculations (Fig. 6) is equal to 2.61 eV and coincides with its experimental value 2.6 eV, which allows us to use these data to calculate the optical functions of Na_2GeSe_3 crystal.

Valence bands have a weak dispersion and form three energetically isolated bundles of bands. Information on the contributions of atomic orbitals to the crystalline states of Na_2GeSe_3 is provided by calculations of the total and local partial densities of states. The distribution profiles of the total density of states, as well as the contributions from the individual states of various atoms for Na_2GeSe_3 are shown in Fig. 7. It follows from the analysis of the energy distribution of local partial densities of states for sodium, germanium and selenium that in each of the three bundles of occupied bands of s - and p -states they give unequal contributions that differ in value from each other. In the valence band of Na_2GeSe_3 , the $4s$ - and $4p$ -states of selenium predominate, and their energy position is significantly different.

The lowest energy bundle of valence bands, located in the energy range from -13.73 to -10.99 eV, is formed mainly by $4s$ -states of selenium atoms. Despite the prevailing nature of $4s$ -states of selenium, hybridization effects of Ge and Se atoms states for this valence subband are noticeable, and it leads to the appearance of contributions of $4s$ -states of germanium atoms, which are mainly localized in the energy region of the four lower bands, and contributions of Ge $4p$ -states into the next bundle of 6 zones having a weak dispersion.

The average bundle of 4 bands following the s -bands of selenium is separated from them by the energy range of 3.20 eV, and it has a width of 2.07 eV and does not overlap with the upper valence subband, thus it forms an isolated subband. This filled subband has a hybrid character and is formed as a result of the overlapping of Ge $4s$ - and Se $4p$ -states, thus playing a significant role in formation of Ge–Se covalent bonds in $[\text{GeSe}_4]$ tetrahedra forming infinite chains.

The upper bundle of occupied zones can be conditionally separated into two parts: the lower part ($-4.42\dots-2.18$ eV) of 12 zones, which has a mixed character with participation of hybridized $4p$ -states of selenium and $4p$ -states of germanium with a slight admixture of s - and p -states of sodium; the upper one ($-2.18\dots0$ eV) containing 20 zones, *i.e.*, is mainly formed by non-bonding $4p$ -orbitals of selenium, which are filled with two electrons (a lone pair), with the admixture of p -, d -states of germanium and s -, p -states of the alkali metal. The top of valence band at the point Γ is formed exclusively by non-bonding $4p_\pi$ -states of selenium (Fig. 8).

A characteristic feature of Na_2GeSe_3 electronic spectrum is the presence of one isolated unoccupied subband, separated by a forbidden energy interval of the width 0.84 eV from subsequent unoccupied zones. The low-energy electron structure of unfilled electron states of sodium selenogermanate is mainly formed by the “mixing” of free p -states of selenium with s - and p -states of germanium and sodium.

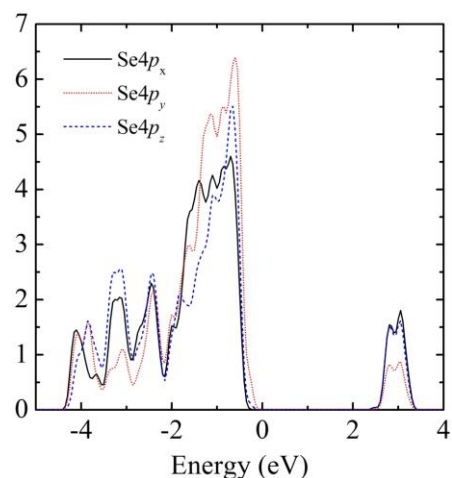


Fig. 8. Dispersion of p -states in selenium.

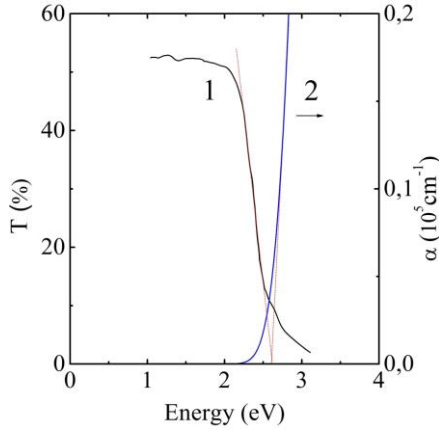


Fig. 9. Experimental transmission spectrum (1) and the calculated absorption one (2) for the Na_2GeSe_3 crystal.

4.2. Optical properties

The energy spectrum of valence electrons directly defines such important characteristics of the crystal as the spectral dependences of the absorption and reflection coefficients. By now, there are only our experimentally measured transmission spectrums in the range of the crystal fundamental absorption edge Na_2GeSe_3 (Fig. 9, curve 1). For comparison of the calculation results with the experimental data on interband absorption, it was of interest to compare behavior of the calculated absorption coefficient $\alpha(\omega)$ near-edge E_g with the experimental transmission spectrum of Na_2GeSe_3 crystal in the range of intrinsic absorption edge, which allowed us to estimate the band gap $E_{gd} = 2.6$ eV (Fig. 9, curve 1). Thus, the theoretically calculated value of $E_{gd} = 2.61$ eV was close to that experimentally determined.

More complete information about the electronic structure of a semiconductor gives a complex of spectra of optical fundamental functions [15]: imaginary (ε_2) and real (ε_1) parts of the dielectric constant; absorption (α) and reflection (R) coefficients; refractive (n) and absorption (k) indices; the real ($\text{Re } \varepsilon^{-1}$, $\text{Re}(1 + \varepsilon)^{-1}$) and imaginary ($-\text{Im } \varepsilon^{-1}$, $-\text{Im}(1 + \varepsilon)^{-1}$) parts of the bulk and surface characteristic losses of electrons, *etc.* In the presence of the experimental reflection spectrum measured in a wide range of energies by using Kramers–Kronig integral relations and corresponding analytical functions, it is possible to calculate the whole complex of optical functions. Since there are no data on the reflection spectrum of Na_2GeSe_3 crystal in a wide energy range, we have performed theoretical calculations of optical functions based on the calculated density of states.

The most important characteristic of the crystal optical response calculation to electromagnetic influence is the complex dielectric function $\varepsilon(\omega) = \varepsilon_1(\omega) + i\varepsilon_2(\omega)$. To calculate the frequency-dependent dielectric function, it is necessary to have its proper values of energy and wave functions of electrons, which are the initial data for the band structure calculation. The imaginary part of dielectric function $\varepsilon_2(\omega)$ in the optical frequency range

was calculated integrating between the occupied and unoccupied electron states, according to the expression:

$$\varepsilon_2(\omega) = \frac{2e^2\pi}{\Omega\varepsilon_0} \sum_{k,V,C} \left| \langle \Psi_k^C | \mathbf{u} \cdot \mathbf{r} | \Psi_k^V \rangle \right|^2 \times \delta(\mathbf{E}_k^C - \mathbf{E}_k^V - \hbar\omega), \quad (1)$$

where Ω is the volume of unit cell, \mathbf{u} – vector determining the polarization of the electric field of light radiation, which is averaged across all spatial directions in the polycrystalline case, \mathbf{k} – reciprocal lattice vector, and $\langle \Psi_k^C | \mathbf{u} \cdot \mathbf{r} | \Psi_k^V \rangle$ – matrix elements that determine the probability of electron transitions from levels \mathbf{E}_k^V in the valence band to levels \mathbf{E}_k^C in the conduction band (transition moments).

The real part of dielectric function $\varepsilon_1(\omega)$ was calculated from the imaginary part of $\varepsilon_2(\omega)$ dependence by using the known Kramers–Kronig relationship:

$$\varepsilon_1(\omega) = 1 + \frac{2}{\pi} \int_0^\infty \frac{\omega' \varepsilon_2(\omega')}{\omega'^2 - \omega^2} d\omega'. \quad (2)$$

Optical constants – refractive n and absorption (coefficient of extinction) k indices – are expressed through the real and imaginary parts of the complex dielectric permittivity in the following way:

$$n^2 - k^2 = \varepsilon_1(\omega), \quad 2nk = \varepsilon_2(\omega), \quad \alpha = \frac{4nk}{\lambda} \quad (3)$$

and are linked by the Kramers–Kronig relationships in the following form:

$$n(\omega) = 1 + P \int_{-\infty}^{\infty} \frac{d(\omega')}{\omega' - \omega},$$

$$k(\omega) = -P \int_{-\infty}^{\infty} \frac{d\omega' n(\omega') - 1}{\pi (\omega' - \omega)}. \quad (4)$$

The reflection coefficient R of light falling normally on the investigated crystal surface is associated with the complex refractive index $n(\omega) = n - ik$ by the ratio:

$$R = \frac{|\bar{n} - 1|^2}{|\bar{n} + 1|^2} = \frac{(n-1)^2 + k^2}{(n+1)^2 + k^2}. \quad (5)$$

Being based on the band structure of Na_2GeSe_3 crystal, the real $\varepsilon_1(\hbar\omega)$ and imaginary $\varepsilon_2(\hbar\omega)$ parts of dielectric function were calculated using the relations (1) and (2), and they are shown in Figs 10a and 10b for three different polarizations of optical radiation ($\mathbf{E} \parallel \mathbf{a}$, $\mathbf{E} \parallel \mathbf{b}$, $\mathbf{E} \parallel \mathbf{c}$). As illustrated in Figs 10a and 10b, the dielectric functions of this crystal have the most significant dependence on the vector \mathbf{E} direction of the electromagnetic wave within the energy range 2.6...12 eV. The significant

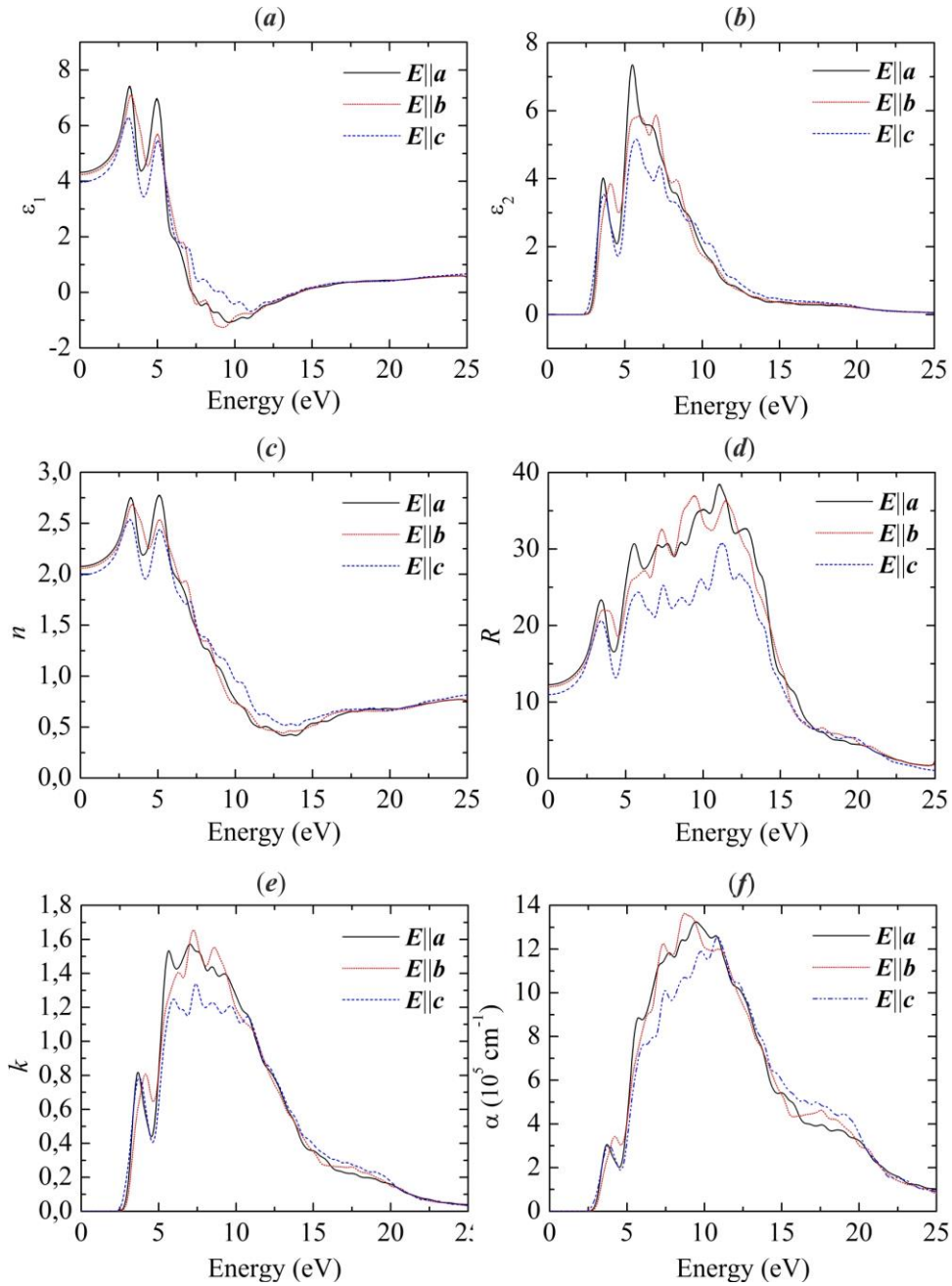


Fig. 10. Real ε_1 (a) and imaginary ε_2 (b) parts of the dielectric function, reflection R (c) and absorption α (d) spectra, absorption k (e) and refraction n (f) coefficients of Na_2GeSe_3 crystal for light polarized along the principal axes a , b , c .

anisotropy of $\varepsilon_2(\hbar\omega)$ within the range 2.6...8 eV is mainly caused by the spatial polarization of the localized electron p -orbitals of selenium forming the upper part of Na_2GeSe_3 valence band (Fig. 8).

The values of static dielectric constant (Fig. 10a) at zero frequency are as follows: $\varepsilon_1^{xx}(0) = 4.319$, $\varepsilon_1^{yy}(0) = 4.239$, $\varepsilon_1^{zz}(0) = 3.967$. The calculated spectrum of $\varepsilon_2(\hbar\omega)$ begins with the energy of 2.61 eV, which defines the position of long-wave edge of this crystal fundamental absorption (Fig. 9, curve 1). With increasing energy, it is observed a sharp growth in ε_2 , which reaches

its maximum value at 3.57 eV in polarization $\mathbf{E}\parallel\mathbf{a}$, then sharply decreases down to its minimum value at 4.5 eV, then again the increase in $\varepsilon_2(\hbar\omega)$ occurs until the second maximum is reached at 5.46 eV, which is followed by a sharp decrease, on which the features in the form of steps are observed. In polarization $\mathbf{E}\parallel\mathbf{b}$, the first maximum in the spectrum of $\varepsilon_2(\hbar\omega)$ is slightly shifted to the high-energy range (4.11 eV), and the features observed in the spectrum of $\varepsilon_2(\hbar\omega)$ in polarization $\mathbf{E}\parallel\mathbf{a}$ in the form of steps, also in polarizations $\mathbf{E}\parallel\mathbf{b}$ and $\mathbf{E}\parallel\mathbf{c}$ appear as maxima. The maximum of $\varepsilon_2(\hbar\omega)$ dependence at the photon

energy $\varepsilon_2 = 3.57$ eV is caused by optical transitions between the upper group of the valence band and the lower separated bundle of unfilled bands (Figs 6 and 7).

The calculated spectral dependences of reflection $R(\hbar\omega)$, excitation $k(\hbar\omega)$, and absorption $\alpha(\hbar\omega)$ coefficients of Na_2GeSe_3 crystal (Fig. 10d, 10e and 10f) well reflect the main features of $\varepsilon_2(\hbar\omega)$ dependence (Fig. 10b). The shape of calculated spectral dependence $n(\hbar\omega)$ and the energy positions of maxima and minima of Na_2GeSe_3 refractive index are in good agreement with maxima and minima on the curve of the real dielectric function $\varepsilon_1(\hbar\omega)$. The calculated values of refractive index $n(\hbar\omega)$ at zero frequency are as follows: $n^{xx}(0) = 2.08$, $n^{yy}(0) = 2.06$, $n^{zz}(0) = 1.99$, and the maximum value falls inside the energy range 2.5...7.5 eV.

Being based on calculations of the electronic structure (Fig. 6) and the density of states (Fig. 7), the existing features in spectra of optical functions within the range 2.5...12 eV can be associated with interband transitions between the levels of the upper valence band formed by p -states of selenium lone pairs and the lower levels of the conduction band. Thus, the maximum at 3.57 eV is caused by the transitions from the top of the valence band formed by $4p$ -states of selenium lone pairs to the lower conduction band formed by hybridized free p -states of selenium and s -, p -states of germanium and sodium. The most intense maximum at 5.46 eV is caused by optical transitions between the middle group of the upper valence band and the lower separated conduction band (Fig. 7).

Thus, both in the reflection spectrum and in Na_2GeSe_3 dielectric functions spectra, the complex structure is observed as associated with optical transitions from the occupied valence bands to the unoccupied conduction bands.

4.3. Spatial distribution of the electron charge

Studying the distribution of the total valence electron charge density $\rho(\mathbf{r})$ in the form of contour maps allowed us to obtain useful information about the nature of chemical bonds in Na_2GeSe_3 both within the same chain and between chains, which is rather difficult to study experimentally in this complex crystal structure. Also, additional information on the nature of ionic conductivity can be obtained from electron density maps.

When constructing electron density contour maps, the decisive factor is the choice of suitable crystal section planes. The short-range tetrahedral structure in Na_2GeSe_3 complicates the representation of contour maps in an accessible 2D format. In this case, it is the most convenient to imagine electronic configurations in a separate $[\text{GeSe}_4]$ tetrahedron in a plane passing through two selenium atoms and one germanium atom, *i.e.*, in the plane along Se–Ge–Se bond lines. Since in $[\text{GeSe}_4]$ tetrahedra linked in the

chain, there exist two bridging (Se–Ge–Se) and two non-bridging (Ge–Se) selenium atoms, it is appropriate to draw two planes: one through the germanium atom and two bridging selenium atoms, and the second one through the germanium atom and two non-bridging selenium atoms. The electron density distribution $\rho(\mathbf{r})$ between the germanium atom and two non-bridging and bridging selenium atoms belonging to the same $[\text{GeSe}_4]$ tetrahedron is illustrated by the electron density maps shown in Figs. 11a and 11b, respectively. From the comparison of contour maps in Figs 11a and 11b, it follows that the maximum of electron density $\rho(\mathbf{r})$ is concentrated inside the $[\text{GeSe}_4]$ tetrahedra near the positions of selenium atoms. In both planes, there are common contours $\rho(\mathbf{r})$, covering the maxima of electron density on selenium and germanium atoms. The only difference is that in the plane passing through non-bridging selenium atoms, there are only common contours covering two selenium atoms and the same germanium atom, and these contours are elongated from each selenium atom only along with one Ge–Se bond line (Fig. 11a). In the plane containing two bridging selenium atoms (Fig. 11b), common contours cover the same bridging selenium atom of $[\text{GeSe}_4]$ tetrahedron and two germanium atoms belonging to two neighboring tetrahedra. As a result, mainly due to the overlap of electron clouds of bridging atoms of selenium and germanium the peculiar chains $\langle \text{GeSe}_3 \rangle_n^{2n-}$ are formed.

Common contours covering the electron density maxima at germanium and selenium atoms characterize the covalent component of the chemical bond. Deformation of contours in the direction of germanium and selenium atoms indicates a predisposition of these directions to formation of sp^3 -hybrid bonding orbitals. In addition to the covalent component of the chemical bond, Na_2GeSe_3 contains ionic and weak van der Waals components. The ionic component is determined by a partial charge density transfer from germanium and sodium atoms to more electronegative selenium atoms.

Sodium atoms localized in an interchain space have no common electron density contours $\rho(\mathbf{r})$ with neighboring anions (selenium atoms). It can be seen from the electron density contour maps of Na_2GeSe_3 crystal (Figs 11c, 11d) that between endless chains of $[\text{GeSe}_4]$ tetrahedra linked by common vertices there are “tunnels” of minimal electron density, which serve as the channels for the movement of Na^+ ions. Thus, weak participation of sodium atoms in formation of electronic states (low charge density around Na^+ ions) and the presence of through “tunnels” between endless chains $\langle \text{GeSe}_3 \rangle_n^{2n-}$ with a very low charge density along the c axis provide high mobility of sodium ions along these channels, and as a result high ionic conduction.

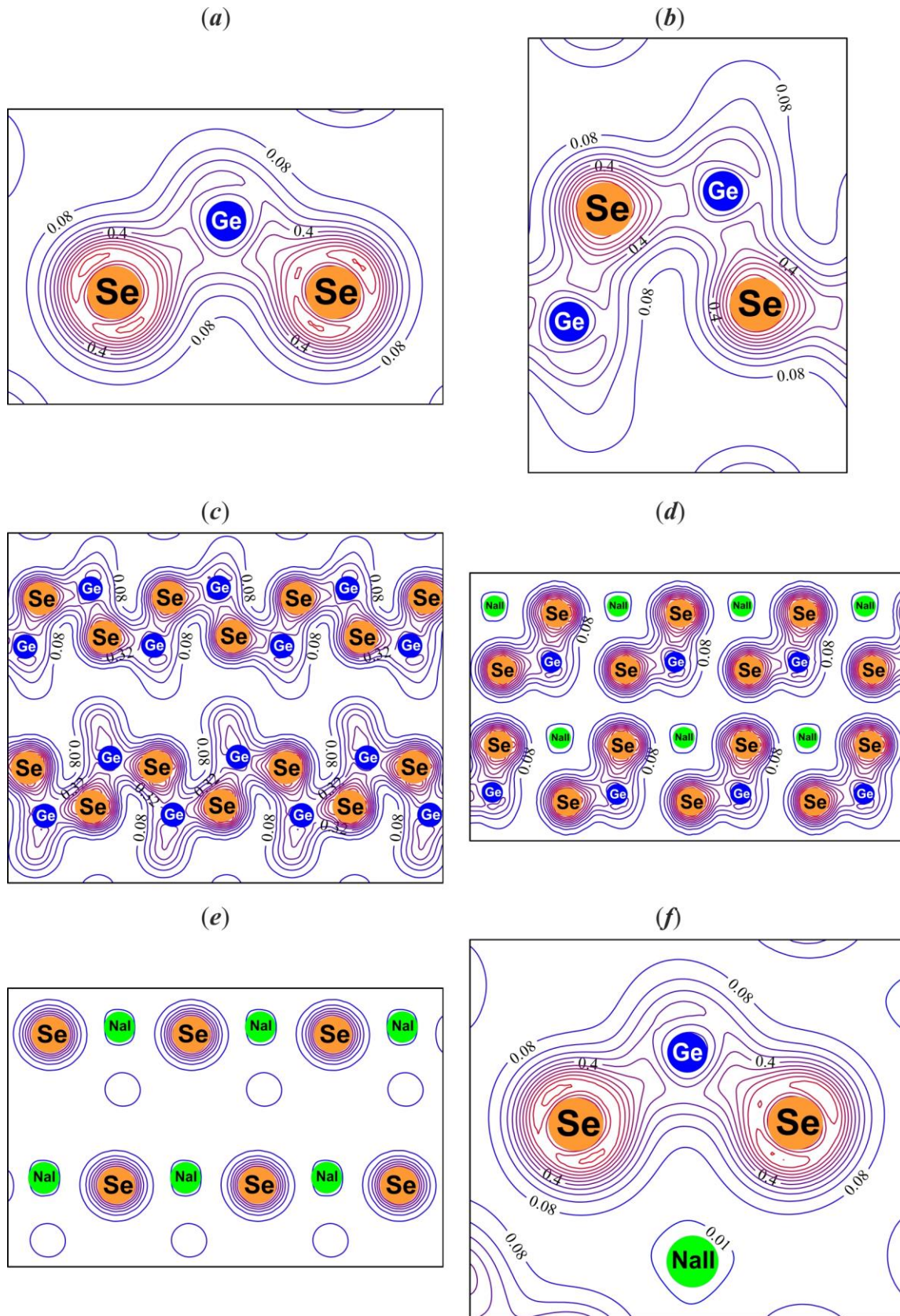


Fig. 11. Maps of the spatial distribution of the charge density in Na₂GeSe₃ crystal at the plane passing: through Ge atom and two non-bridging (a) or two bridging (b) Se atoms in the same [GeSe₄] tetrahedron; along Se–Ge–Se bonds in endless chains (c); through atoms of selenium, germanium, and sodium (d) in Na₂GeSe₃.

5. Conclusions

An original method has been developed for the synthesis of Na_2GeSe_3 compound by fusion of the corresponding stoichiometric amounts of the alkali metal, germanium mono- or diselenide (in the form of a specially made crucible, inside which the alkali metal was placed) and selenium according to the certain regime, which prevents explosion and avoids destruction of the container during the reaction of sodium with germanium selenides and selenium. The Bridgman method was used for growing Na_2GeSe_3 single crystals of high optical quality.

The *ab initio* method of the density functional in the LDA+*U* approximation, the energy band structure, total and partial densities of states, spatial distribution of the electron density, and optical functions of the Na_2GeSe_3 crystal were calculated. Sodium selenogermanate is a direct-gap semiconductor with the calculated band gap $E_{gd} = 2.61$ eV, which is in good agreement with the experimental value $E_g = 2.6$ eV determined from the analysis of the optical absorption edge.

From the analysis of electron density distribution maps of Na_2GeSe_3 crystal, it follows that the chemical bond between the cation (germanium) and the anion (selenium) in endless chains has a covalent-ionic character, and the chains are linked to each other by weak van der Waals forces. The low charge density around Na^+ ions and the presence of through “tunnels” between endless chains provide high mobility of sodium ions along these channels and, as a result, the high ionic conductivity of the crystal and glass.

References

- Gandi S., Vaddadi V.S.C.S., Panda S.S.S. *et al.* Recent progress in the development of glass and glass-ceramic cathode/solid electrolyte materials for next-generation high capacity all-solid-state sodium-ion batteries: A review. *J. Power Sources*. 2022. **521**. P. 230930. <https://doi.org/10.1016/j.jpowsour.2021.230930>.
- Wang Y., Song S., Xu C. *et al.* Development of solid-state electrolytes for sodium-ion battery – A short review. *Nano Mater. Sci.* 2019. **1**, No 2. P. 91–100. <https://doi.org/10.1016/j.nanoms.2019.02.007>.
- Barrau B., Ribes M., Maurin M., Kone A., Souquet J.-L. Glass formation, structure and ionic conduction in the Na_2S – GeS_2 system. *J. Non-Cryst. Sol.* 1980. **37**. P. 1–14. [https://doi.org/10.1016/0022-3093\(80\)90473-1](https://doi.org/10.1016/0022-3093(80)90473-1).
- Kim S.K., Mao A., Sen S., Kim S. Fast Na-ion conduction in a chalcogenide glass-ceramic in the ternary system Na_2Se – Ga_2Se_3 – GeSe_2 . *Chem. Mater.* 2014. **26**, No 19. P. 5695–5699. <https://doi.org/10.1021/cm502542p>.
- Plumat E.R. New sulfide and selenide glasses: preparation, structure, and properties. *J. Amer. Ceramic Society*. 1968. **51**. P. 499–507. <https://doi.org/10.1111/j.1151-2916.1968.tb15675.x>.
- Eisenmann B., Hansa J., Schaefer H. Zur Kenntnis der Selenidosilikate und -germanate $\text{Na}_4\text{Si}_4\text{Se}_{10}$, Na_2GeSe_3 und $\text{Na}_8\text{Ge}_4\text{Se}_{10}$. *Z. Naturforsch. B.* 1985. **40**, No 4. P. 450–457. <https://doi.org/10.1515/znb-1985-0402>.
- Chung I., Song J.-H., Jang J. I., *et al.* $\text{Na}_2\text{Ge}_2\text{Se}_5$: A highly nonlinear optical material. *J. Solid State Chem.* 2012. **195**. 161–165. <https://doi.org/10.1016/j.jssc.2012.05.038>.
- Cheng X.-D., Wu H.-X., Tang X.-L., *et al.* First principles study on the electronic structures and optical properties of $\text{Na}_2\text{Ge}_2\text{Se}_5$. *Acta Phys. Sin.* 2014. **63**, No 18. P. 184208-1–184208-7. <https://doi.org/10.7498/aps.63.184208>.
- Dittmar G., Schäfer H. Die Kristallstruktur von germanium diselenid. *Acta Crystallogr. B.* 1976. **32**. P. 2726–2728. <https://doi.org/10.1107/S0567740876008704>.
- Kohn W. Nobel Lecture: Electronic structure of matter-wave functions and density functionals. *Rev. Mod. Phys.* 1999. **71**. P. 1253–1266. <https://doi.org/10.1103/RevModPhys.71.1253>.
- Himmetoglu B., Floris A., de Gironcoli S., Cococcioni M. Hubbard-corrected DFT energy functionals: The LDA+*U* description of correlated systems. *Int. J. Quantum Chem.* 2014. **114**. P. 14–49. <https://doi.org/10.1002/qua.24521>.
- García A., Papior N., Akhtar A. *et al.* Siesta: Recent developments and applications. *J. Chem. Phys.* 2020. **152**, No 20. P. 204108-1–204108-31. <https://doi.org/10.1063/5.0005077>.
- Hartwigsen C., Goedecker S., Hutter J. Relativistic separable dual-space Gaussian pseudopotentials from H to Rn. *Phys. Rev. B.* 1998. **58**. P. 3641–3662. <https://doi.org/10.1103/PhysRevB.58.3641>.
- Monkhorst H.J., Pack J.D. Special points for Brillouin-zone integrations. *Phys. Rev. B.* 1976. **13**. P. 5188–5192. <https://doi.org/10.1103/PhysRevB.13.5188>.
- Yu P. and Cardona M. *Fundamentals of Semiconductors: Physics and Materials Properties*. Springer, Berlin, 2010. <https://link.springer.com/content/pdf/10.1007%2F978-3-642-00710-1.pdf>.

Authors and CV



Dmytro I. Bletska, born in 1946, defended his Doctoral Dissertation in Physics and Mathematics in 1985 and became full professor in 1988. Professor of the department physics of semiconductors at Uzhhorod National University, Ukraine. Authored over 260 scientific publications, 86 patents, 2 textbooks, 2 monographs. The area of his scientific interests – technology and the physics of highly anisotropic layered crystals, physical properties of chalcogenide glassy semiconductors and superionics. ORCID: <https://orcid.org/0000-0003-1816-8787>. E-mail: dmytro.bletska@uzhnu.edu.ua



Vasyl V. Vakulchak, born in 1986, defended his PhD thesis in Physics and Mathematics in 2015. Senior researcher of the department of Applied Physics at Uzhhorod National University, Ukraine. Authored of 80 scientific publications and 1 patents. The area of scientific interests is *ab-initio* calculation of the electronic structure, physical properties of semiconductors.

ORCID: <https://orcid.org/0000-0001-6037-8978>.

E-mail: vasyi.vakulchak@uzhnu.edu.ua



Oksana A. Mykaylo, born in 1963, defended her PhD thesis in Physics and Mathematics in 1994 and became senior researcher of the department of Applied Physics at Uzhhorod National University in 2001. Authored more than 70 scientific publications, 2 patents and the monograph. The area of scientific interests is physical-chemical properties of semiconductors and aerogels.

E-mail: oksanamykaylo@gmail.com



Igor L. Mykaylo, born in 1963, defended his PhD thesis in Chemistry in 1991 at the Institute of General and Inorganic Chemistry of the Russian Academy of Sciences, Moscow. Authored more than 30 scientific publications, 4 patents. The area of scientific interests is the

growth and physical-chemical properties of semiconductors. E-mail: crystal_lab457@yahoo.com

Author contribution

Bletskan D.I.: Conceptualization, Writing - Original draft, Project administration.

Vakulchak V.V. : Software, Validation, Investigation, Supervision.

Mykaylo I.L. : Methodology, Investigation, Resources.

Mykaylo O.A.: Resources, Writing - Review & Editing.

Отримання, електронна структура та оптичні властивості кристалів Na_2GeSe_3

Д.І. Блецкан, В.В. Вакульчак, І.І. Михайло, О.А. Михайло

Анотація. З перших принципів у рамках теорії функціонала густини у LDA та LDA+*U*-наближеннях проведено розрахунки зонної структури, повної і парціальної густин електронних станів, просторового розподілу густини електронного заряду та оптичних функцій: діелектричної проникності, показників заломлення та поглинання, коефіцієнтів відбивання та поглинання Na_2GeSe_3 . За результатами розрахунку Na_2GeSe_3 є прямозонним кристалом із вершиною валентної зони та дном зони провідності у точці Γ зони Бриллюена. Розрахована ширина забороненої зони становить $E_{gd} = 1.7$ eВ в LDA і $E_{gd} = 2.6$ eВ у LDA+*U*-наближенні. За даними повної і парціальних густин електронних станів визначено вклади атомних орбіталей у кристалічні орбіталі, а також отримано дані про формування хімічного зв'язку у досліджуваних кристалах.

Ключові слова: кристалічна структура, вирощування монокристалів, комп'ютерне моделювання, електронна структура, край поглинання, оптичні функції.